

Direct observation of resonant tunneling in heterostructure with a single quantum well

V. I. Zubkov^{1,a)}, Ia. V. Ivanova¹, M. Weyers²

AFFILIATIONS

¹*St. Petersburg State Electrotechnical University "LETI", Professor Popov Street 5, 197376, St. Petersburg, Russia*

²*Ferdinand-Braun-Institut gGmbH, Leibniz-Institut für Höchstfrequenztechnik, Gustav-Kirchhoff-Str. 4, D-12489 Berlin, Germany*

^{a)}Author to whom correspondence should be addressed: vzubkovspb@mail.ru

ABSTRACT

A resonant-tunneling conductivity was experimentally registered in doped heterostructure with a single quantum well using admittance spectroscopy. Earlier this effect was only realized in artificially created resonant tunneling structures, having four heterojunctions. A heterostructure with $\text{In}_{0.3}\text{Ga}_{0.7}\text{As}/\text{GaAs}$ quantum well was examined in temperature range 10 – 300 K. In admittance spectra a competition of thermionic and tunneling escape mechanisms was noticed with non-exponential Arrhenius plot. By means of numerical self-consistent simulations in a quantum box we have shown the role of a quasi-bound level in resonant tunneling of electrons; in addition the energies and wave functions of the quasi-bound state were derived in dependence on applied bias. The modification of transparency coefficient for two-barrier Hartree potential as a function of quantum well width and in dependence on applied bias was also calculated. The resonant state took place only at symmetric barriers and disappeared, when the electric field tilted the barriers. The results can be used to develop a new type of resonant tunneling diodes, and as a method for diagnostics of tunnel effect in semiconductors.

A resonant-tunneling conductivity in a doped heterostructure with a single quantum well (QW) was experimentally observed by admittance spectroscopy. Before, this effect was only realized in specially designed resonant tunneling structures, where the movement of electrons with positive energy through tunnel-transparent composite barriers was implemented.^{1–3} In our experiment, it appears as strong increasing ac conductance at a certain QW width and near zero applied bias. This effect occurs when the energy of the quasi-bound level in the quantum well, which is pushed out to the continuous spectrum, coincides with the eigenenergies of a “resonator”, formed by doped layers of the double heterostructure around the QW. The observation conditions are low temperature, identical doping of the QW adjacent layers and a relatively large energy band offset.

We study a heterostructure with an elastically-strained $\text{In}_x\text{Ga}_{1-x}\text{As}/\text{GaAs}$ ($x=0.3$) quantum well.^{4,5} Previously, the considered effect was not detected in experiments, since the detailed studies, as well as modeling in these quantum wells were typically limited to In-content $x = 0.15 - 0.25$, traditionally used in optoelectronic devices in this heterosystem.

Certainly, numerous theoretical simulations have been devoted to energy states in a single quantum well heterostructure, starting with the classical early works,^{6–10} and including a number of specialized free-ware solvers developed in recent decades by various universities (e.g.^{11,12}). Add here the computing resources of nanoHUB simulation gateway and TCAD Synopsys software. As a rule,

the implemented models consider separately bound states in QW and the continuous energy spectrum above it. Within the separate solution of these problems it is not possible to correctly determine the energy of a quasi-bound state at $E > 0$ and its behaviors upon the external conditions change.

The article starts with presenting original experimental results that demonstrates the tunnel-resonance conductivity in a doped heterostructure with only two heterojunctions, rather than four, as in a conventional resonant tunneling diode (RTD). Next, a numerical self-consistent calculation of energy and wave functions of the bound ($E < 0$) and quasi-bound ($E > 0$) states in the quantum well is performed, as well as their modification against the bias applied to the structure. The third part is devoted to modeling the transparency coefficient of the two-barrier structure. The conditions of effective resonant tunneling for electrons are also analyzed here.

The equipment used for this study includes LCR-meter Agilent E4980A, Janis CCR-10 cryogenic probe station, and LakeShore temperature controller.¹³ The available temperature range is 10 – 450 K. Heterostructures with a single GaAs/In_xGa_{1-x}As/GaAs QW in the composition range $x = 0.15 \dots 0.30$ were grown by metalorganic vapor phase epitaxy (MOVPE) on *n*-GaAs substrates. Care was taken to have the same doping level in the barrier layers on both sides. For this study a sample with quantum well of $x=0.3$ and width $w=6.8$ nm was selected, Fig. 1(a). High-resolution X-ray diffraction was applied to determine layer thickness w and indium content x in QW by comparing the measured rocking curves to simulated ones. We estimate the error in thickness w as less than 0.25 nm and the composition error as $\Delta x = \pm 0.0025$ for QWs investigated in the work ($x = 0.20 \dots 0.30$).⁴

The thickness of the cap-layer over the quantum well was > 300 nm, so the electric field did not penetrate the QW region until -2.2 V bias was applied to the contacts, Fig. 1(b).

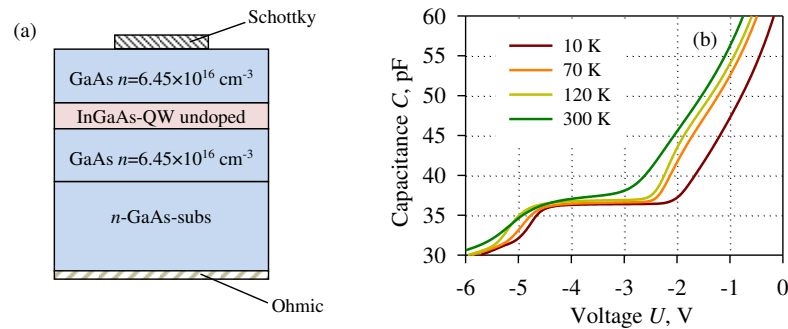


Fig. 1. (a) A sketch of the sample structure. (b) C-V characteristics of GaAs/In_{0.3}Ga_{0.7}As/GaAs QW ($w = 6.8$ nm) at different temperatures. Test signal frequency $f = 1$ MHz.

In the temperature conductance spectra $G/\omega - T$, taken at different frequencies, we have observed a combined signal that experienced strong modification with applied bias (Fig. 2). First of all, there was a thermionic contribution of conductance, resembling a Gaussian-like curve; the specific feature of this component is the frequency dependence of the temperature peak (Fig. 2(b), bias -2.3 V). In addition, on the low temperature side, a slightly temperature-dependent tunneling component of conductance was observed. With the increase of reverse bias from zero, the amplitude of the tunnel plateau experiences a sharp drop, in the region of -2.3 V (at the maximum of thermionic conductance) it reaches a minimum, and then the plateau slightly rises again. We suppose that on top of thermally activated emission, two types of charge carrier tunneling from the quantum well there pre-

sent: 1) ordinary tunnel escape through a single triangular barrier at large reverse bias (Fig. 2(c)), and 2) resonant tunneling via two symmetric potential barriers (Fig. 2(a)) at near zero biases.

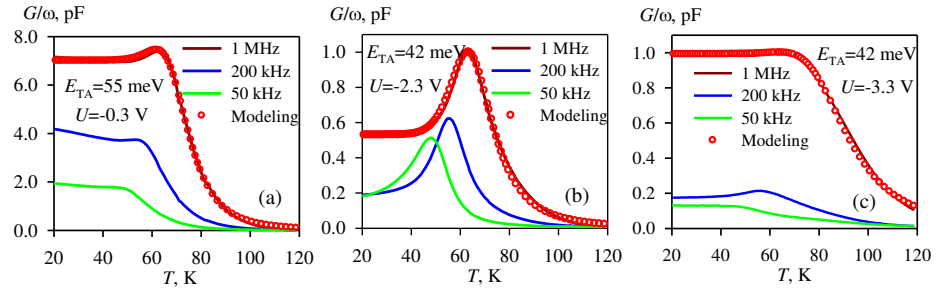


Fig. 2. Experimental spectra $G/\omega-T$ at biases: (a) -0.3 V, (b) -2.3 V, (c) -4.3 V. Red open circles – modeled spectra at frequency 1 MHz.

This assumption is confirmed by measurements of frequency-dependent conductance of the structure against the applied bias ($G/\omega-U$), Fig. 3(a). At first (small reverse biases), there is two-barrier resonant tunneling, then (starting at about -1.7 V) the symmetry of the barriers begins to break, and the amplitude of the resonant-tunneling component drops sharply, compared with the amplitude of the thermionic emission. The peak at -4.7 V at the end of the plateau relates to incoherent thermally activated tunneling through a single triangular barrier.¹⁴

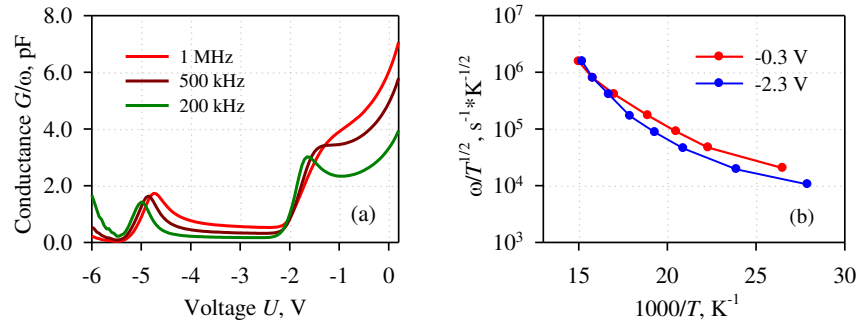


Fig. 3. (a) Active conductance at 32 K as function of applied bias. (b) Arrhenius plots constructed on conductance spectra Fig. 2.

Analysis of the experimental spectra allows estimating the activation energy E_A of the process and its velocity via building the Arrhenius plot in coordinates ω (or, more correctly, $\omega/T^{1/2}$) vs. $1000/T$. At this, for the maximum of the spectrum the condition is fulfilled¹⁵

$$\omega = e_n, \quad (1)$$

where e_n is the thermal emission rate for charge carriers from the size quantization level in the well:¹⁶

$$e_n = AT^{1/2} \exp(-E_A/kT), \quad (2)$$

with A as a pre-exponential factor.¹⁷

Arrhenius plots (Fig. 3(b)) showed significant deviation from classical representations and were curvilinear due to strong contribution of the tunneling. In this regard, the method of deriving E_A from the slope of the Arrhenius plot turns out to be incorrect, giving only the rough estimation.

It is more correct to determine the emission rates and the parameters E_A and A in (2) by simulation of the conductance spectra and fitting to the experiment. The spectra of Fig. 2 are formed from two components: the tunnel component prevails in the left, low-temperature part, and the thermionic component prevails on the right. Implying the tunneling emission rate of charge carriers from a quantum well is weakly dependent on temperature,¹⁸ we consider it constant for a fixed bias. The thermal activation component can be calculated using the standard expression for a deep center conductance at frequency ω ¹⁵

$$G_{TA}(T) = K \frac{e_n(T)\omega^2}{e_n^2(T) + \omega^2}, \quad (3)$$

where factor K contains information about the concentration of recharged centers, the capacitance of the structure, etc. The activation energy E_A , determined from the Arrhenius graph, is used as zero approximation for the calculations.

With the competition between two channels, the total electron emission rate from the QW can be represented as the sum of the thermal activation e_n^{TA} and tunneling e_n^{tun} emission rates:

$$e_n = e_n^{TA} + e_n^{tun}. \quad (4)$$

Calculated spectra are represented in Figs. 2 by open circles. They match well the experimental ones. Starting from 45 K the thermionic component (3) dominates over the tunnel emission. Fitting by (4) demonstrates the 2.5 times drop of e_{tun} with increasing the applied bias from -0.3 V to -2.3 V.

The quasi-bound state of electrons in the quantum well plays the core role in the resonant tunneling passing of electrons through the barrier.¹⁹ This is its fundamental difference from the pure bound state ($E < 0$), which forms the equilibrium concentration of electrons in the QW. To determine the bound and quasi-bound state energies, we used a numerical simulation, including the calculation of spatial distribution of electrostatic Hartree potential, wave functions and electron concentration in corresponding subbands of the quantum well.

The calculation procedure consists in self-consistent numerical solution of Poisson and Schrödinger equations in the effective mass approximation. The details of the simulation are described in articles.^{17,20} Its principal feature is that a "quantum box" is used to calculate the entire concentration of charge carriers (both bound and free) in the quantum well region. The quantum box represents a region with infinitely high barriers²¹ that includes the quantum well and some area around it, where bound and free states are calculated in one way. Just its use makes it possible to correctly account for states in the region of curved barriers at $E > 0$ and study the effects related to the quasi-bound state.^{22,23} Otherwise, under the assumption of an abrupt 2D – bulk crossover the agreement between experiment and theory get worst at low fields, as shown in work.²⁴

The calculations show that, in contrast to a rectangular potential, in doped heterostructure the second quantization level locates at a positive energy, but below the top of the potential barriers, and its wave function is mostly concentrated in the quantum well. This level becomes *quasi-bound* (or *quasi-stationary*, since it has a finite lifetime²⁵). Far beyond the induced barriers, its wave function

This is the author's peer reviewed, accepted manuscript. However, the online version of record will be different from this version once it has been copyedited and typeset.

PLEASE CITE THIS ARTICLE AS DOI: 10.1063/1.50056842

behaves as for a free state. Note that such states, falling into the continuous spectrum of a semiconductor free band, are also called quasi-resonant states.

Next, we will monitor the quasi-bound state. Fig. 4 shows the Hartree potential distribution $q\phi(x)$ for the structure; it also shows the bound and quasi-bound levels and wave functions of the quasi-bound level for composition $x = 0.3$ at different applied biases. The size of the quantum box $L = 13 \times w$, with the QW is placed in the center.

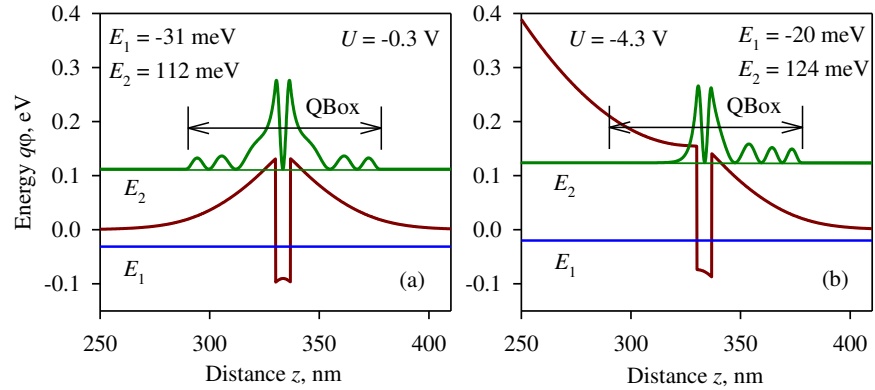


Fig. 4. Potential distribution in $\text{In}_{0.3}\text{Ga}_{0.7}\text{As}/\text{GaAs}$ heterostructure at biases U : (a) -0.3 V, (b) -4.3 V. The positions at 70 K are shown of the bound E_1 and quasi-bound E_2 level and the square of the wave function for the latter one.

While $|U| < 2$ V (case a), the self-consistent potential of the doped heterostructure forms two symmetrical potential barriers at $E > 0$. The wave function for the quasi-bound state is also symmetrical. In case (b) the QW potential is distorted by the applied field, and a triangular potential barrier is formed. Here the wave function becomes essentially asymmetric, penetrating into the region with lowered potential barrier.

Further we calculate the tunnel transparency of the two-sided potential barrier, formed by the doped heterostructure around the quantum well. The simulations were performed using the method of numerical solution for an inner problem.²⁶ The essence of the method is to determine the characteristics of electron scattering at the barrier via its wave function in the inner region of the quantum box ($0 < x < L$), which was taken as before. If the internal problem is solved, the reflection and transmission coefficients can be found. Crucially, the transmission calculations use the Hartree potential, obtained in the above self-consistent calculations.

As a result, there are two different cases.

1. There is no electric field in the quantum well (up to -2.2 V). Here a two-barrier symmetric potential is formed around the QW. Under these conditions, the resonant electron tunneling takes place with participation of the quasi-bound level.²⁷ The narrow transparency channel in Fig. 5(a) is located at about 118 meV. Importantly, if there is different impurity concentration in the barriers and the symmetry of the barriers is broken, then resonant tunneling is not observed.

2. At reverse bias > 2.3 V, the field penetrates into the QW. As the electric field increases, the symmetry of the barriers is broken, and a single triangular potential barrier is formed along with the

This is the author's peer reviewed, accepted manuscript. However, the online version of record will be different from this version once it has been copyedited and typeset.

PLEASE CITE THIS ARTICLE AS DOI: 10.1063/1.50056842

gradual disappearance of the peak of resonant tunneling (the gray curve in Fig. 5(a)). In this case there is a simple tunneling of electrons from the well through the second quantization subband.^{18,28}

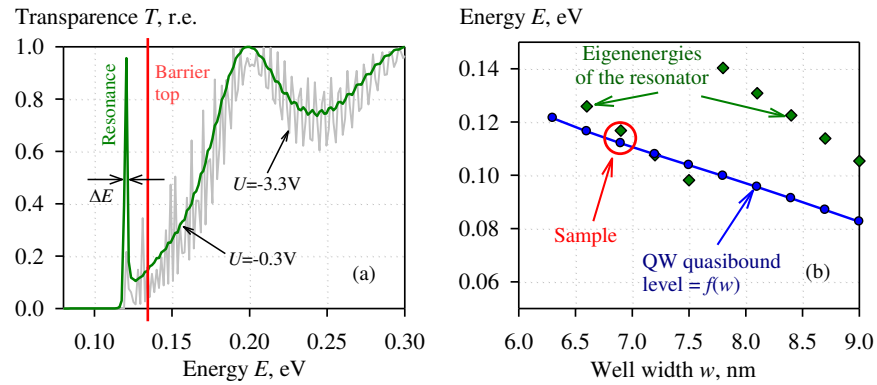


Fig. 5. (a) Calculated transparency coefficient for two-barrier potential of the doped heterostructure with QW at biases -0.3 V (green line) and -3.3 V (gray line). The red line is the position of the potential barrier top (~ 130 meV). (b) Dependence of the quasi-bound level (blue circles) and the eigenenergies for the barrier resonator (green squares) on the QW width. The calculations are made for 70 K and -0.3 V bias. Red circle represents sample under study.

The performed calculations demonstrate the periodicity of the observed resonance pattern: the appearance, shift, smearing and disappearance of the resonant peak with decrease of the QW width. Its position is shown by green squares in Fig. 5(b). So, the eigenenergy for the resonator is a periodic function of the QW width, experiencing an abrupt change at certain values. The period of the mode jump is 1.7 nm.

In contrast, the quasi-bound level always exists down to $w \sim 1.7$ nm, and its energy monotonically decreases with the expansion of the well, Fig. 5(b). When its energy coincides with the resonator eigenenergy (at $w = 7$ nm), an extremely thin tunneling transparency peak does appear. The peak is expanding rapidly upon the well narrowing from 7.0 to 6.6 nm, moves and then disappears. The next peak arises after 1.7 nm.

As can be seen from Fig. 5(b), for the studied sample with QW width of 6.8 nm, the quasi-bound level is close to the transparency channel of the two-barrier potential. This means that in this sample there are conditions for high-efficiency resonant tunneling conductivity.

Analyzing the FWHM (or ΔE) for the resonant peaks, one can estimate the tunneling time constant, basing on the uncertainty relation $\Delta E \times \Delta t = h$. The corresponding time constant is varied from 0.084 ps (at $w = 6.6$ nm) up to 457 ps at 7.2 nm.

Important, the resonance conditions disappear if the impurity concentrations in the barriers differ by more than $\sim 10\%$. Besides, at In content $x < 0.27$ a small band offsets form weak barriers, and the thermionic escape dominates.

Resonant electron tunneling is usually compared to the phenomenon of resonant transparency of optical Fabry–Perot interferometer, which occurs when the distance between mirrors is equal to an integer number of half-waves. In resonant tunneling structure, this is analogous to the equality of the distance between the barriers to an integer number of de Broglie half-waves. And this, in turn, corresponds to the occurrence of a quasi-stationary state for electronic waves.²⁹

Thus, one can directly determine the de Broglie wavelength of an electron from the experiment. It turns out to be equal to the half of the observed period, i.e. 0.85 nm.

The discovered effect is principally different from the known implementations of resonant tunneling diodes (RTD). The traditional RTD is a nanostructure comprised of four heterojunctions, where a “quantum well” is enclosed between two tunneling-transparent barrier regions 1.5–5 nm thick. In this paper, in contrast, we do observe the resonant-tunneling effect in a structure having only two heterojunctions, without specially grown thin barrier layers. Here the symmetric two-barrier electrostatic potential is self-formed in the doped regions adjacent to the well. The ability to detect and analyze this effect in detail is provided by low-temperature measurements of admittance spectra and corresponding numerical simulations of quantum-sized structure.

Thus, the effect of resonant-tunneling conductivity was detected experimentally by methods of admittance spectroscopy and confirmed theoretically. The results of numerical simulation fill the gap between discrete and continuous spectra and give the tool to observe the field dependent modification of the quasiresonance state. They characterize in detail the resonant-tunneling mechanism of ac conductivity in a doped heterostructure with a single quantum well and the conditions for its observation.

The resonant tunneling structure on heterostructure with two heterojunctions will possess simpler technology with the only requirement of the identity of impurity concentration in QW barriers. Due to the strong dependence of its characteristics on the barrier symmetry, the proposed resonant tunneling structure can be used where high sensitivity is required, rather than high power.

The results of the study can be used also as a method for diagnostics of tunnel effect in semiconductor quantum wells by admittance spectroscopy.

ACKNOWLEDGMENTS

The authors express deep gratitude to Dr. F. Bugge (FBI, Berlin) for samples fabrication, Prof. G. F. Glinskii (St. Petersburg ETU “LETI”) and Prof. A. M. Satanin (University of Nizhny Novgorod) for their valuable comments and discussion.

DATA AVAILABILITY

The data that support the findings of this study are available from the corresponding author upon reasonable request.

REFERENCES

- ¹L. L. Chang, L. Esaki, R. Tsu, *Appl. Phys. Lett.* **24**, 593 (1974).
- ²L. V. Keldysh, *Her. Russ. Acad. Sci.* **86**, 413 (2016).
- ³P. Ontay, A. Amthong, *Eur. J. Phys.* **40**, 035403 (2019).
- ⁴F. Bugge, U. Zeimer, M. Sato, M. Weyers, G. Tränkle, *J. Cryst. Growth* **183**, 511 (1998); F. Bugge, U. Zeimer, S. Gramlich, I. Rechenberg, J. Sebastian, G. Erbert, M. Weyers. *J. Cryst. Growth* **221**, 496 (2000).
- ⁵M. Weyers, A. Bhattacharya, F. Bugge, A. Knauer, *Topics Appl. Phys.* **78**, 83 (2000).
- ⁶F. Stern, *Phys. Rev. B* **5**, 4891(1972).

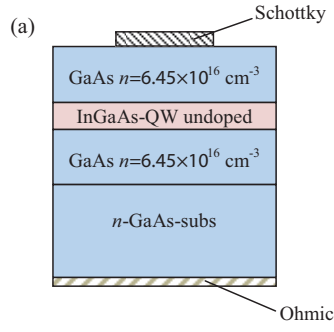
This is the author's peer reviewed, accepted manuscript. However, the online version of record will be different from this version once it has been copyedited and typeset.

PLEASE CITE THIS ARTICLE AS DOI: 10.1063/1.50056842

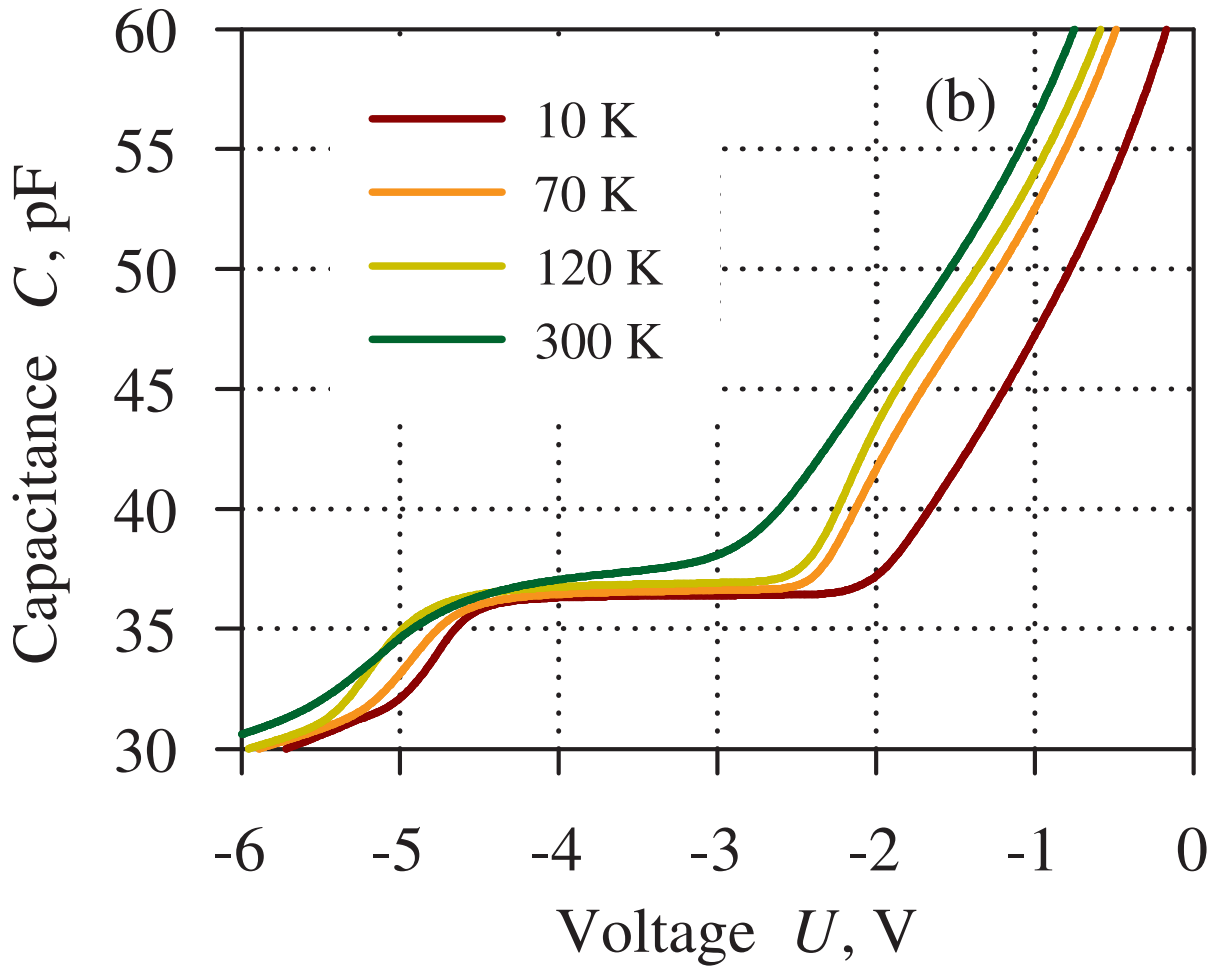
- ⁷I.-H. Tan, G. L. Snider, L. D. Chang, E. L. Hu, J. Appl. Phys. **68**, 4071 (1990).
- ⁸G. L. Snider, I.-H. Tan, E. L. Hu, J. Appl. Phys. **68**, 2849 (1990).
- ⁹P. N. Brounkov, T. Benyattou, G. J. Guillot, J. Appl. Phys. **80**, 864 (1996).
- ¹⁰E. Cassan, J. Appl. Phys. **87**, 7932 (2000).
- ¹¹M. Grupen, K. Hess, IEEE J. Quantum Electron. **34**, 120 (1998).
- ¹²M. Ghosh, S. Ghosh, A. Acharyya, J. Comput. Electron. **15**, 1370 (2016).
- ¹³V. I. Zubkov, O. V. Kucherova, S. A. Bogdanov, A. V. Zubkova, J. E. Butler, V. A. Ilyin, A. V. Afanas'ev, A. L. Vikharev, J. Appl. Phys. **118**, 145703 (2015).
- ¹⁴K. Schmalz, I. N. Yassievich, H. Rucker, H. G. Grimmeiss, H. Frankenfeld, W. Mehr, H. J. Osten, P. Schley, and H. P. Zeindl, Phys. Rev. B **50**, 14287 (1994).
- ¹⁵G. Vincent, D. Bois, P. Pinard, J. Appl. Phys. **46**, 46 (1975).
- ¹⁶N. Debbar, D. Biswas, P. Bhattacharya, Phys. Rev. B **40**, 1058 (1989).
- ¹⁷V. I. Zubkov, M. A. Melnik, A. V. Solomonov, E. O. Tsvelev, F. Bugge, M. Weyers, G. Tränkle, Phys. Rev. B **70**, 075312 (2004).
- ¹⁸M. Geller, A. Marent, E. Stock, D. Bimberg, V. I. Zubkov, I. S. Shulgunova, A. V. Solomonov, Appl. Phys. Lett. **89**, 232105 (2006).
- ¹⁹J. A. Berashevich, V. E. Borisenko, J.-L. Lazzari, F. A. D'Avitaya, Phys. Rev. B **75**, 115336 (2007).
- ²⁰V. I. Zubkov, Semicond. **40**, 1204 (2006).
- ²¹L. I. Schiff, *Quantum Mechanics* (McGraw-Hill, 1968).
- ²²V. I. Zubkov, Semicond. **41**, 320 (2007).
- ²³S. Rihani, H. Page, H. E. Beere, Superlattices Microstruct. **47**, 288 (2010).
- ²⁴J. Nelson, M. Paxman, K.W. J. Barnham, J.S. Roberts, and C. Button. Steady-state carrier escape from single quantum wells. IEEE J. Quantum Electronics, **29**, 1460 (1993).
- ²⁵V. Y. Aleshkin, L. V. Gavrilenko, M. A. Odnoblyudov, Y. N. Yassievich, Semicond. **42**, 880 (2008).
- ²⁶C. S. Kim, A. M. Satanin, and V. B. Shtenberg, Semicond. **36**, 539 (2002).
- ²⁷A. Messiah, *Quantum Mechanics* (Dover Publications, 1999).
- ²⁸M. Geller, E. Stock, R. L. Sellin, D. Bimberg, Physica E **32**, 171 (2006).
- ²⁹W. van Haeringen, D. Lenstra, *Analogies in Optics and Micro Electronics* (Kluwer Academic Publishers, Dordrecht, 1990).

This is the author's peer reviewed, accepted manuscript. However, the online version of record will be different from this version once it has been copyedited and typeset.

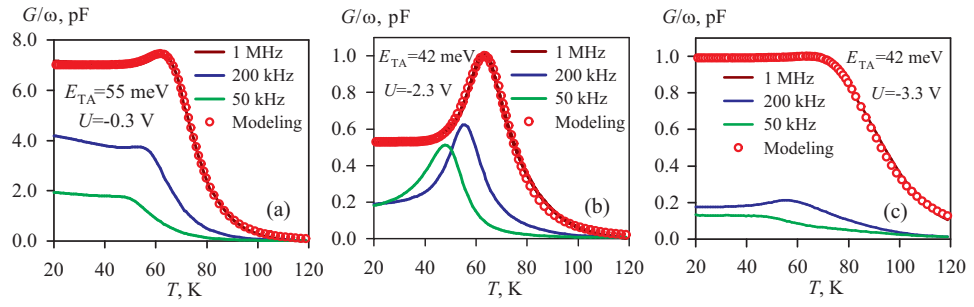
PLEASE CITE THIS ARTICLE AS DOI: 10.1063/1.50056842



This is the author's peer reviewed, accepted manuscript. However, the online version of record will be different from this version once it has been copyedited and typeset.
PLEASE CITE THIS ARTICLE AS DOI: 10.1063/1.50056842

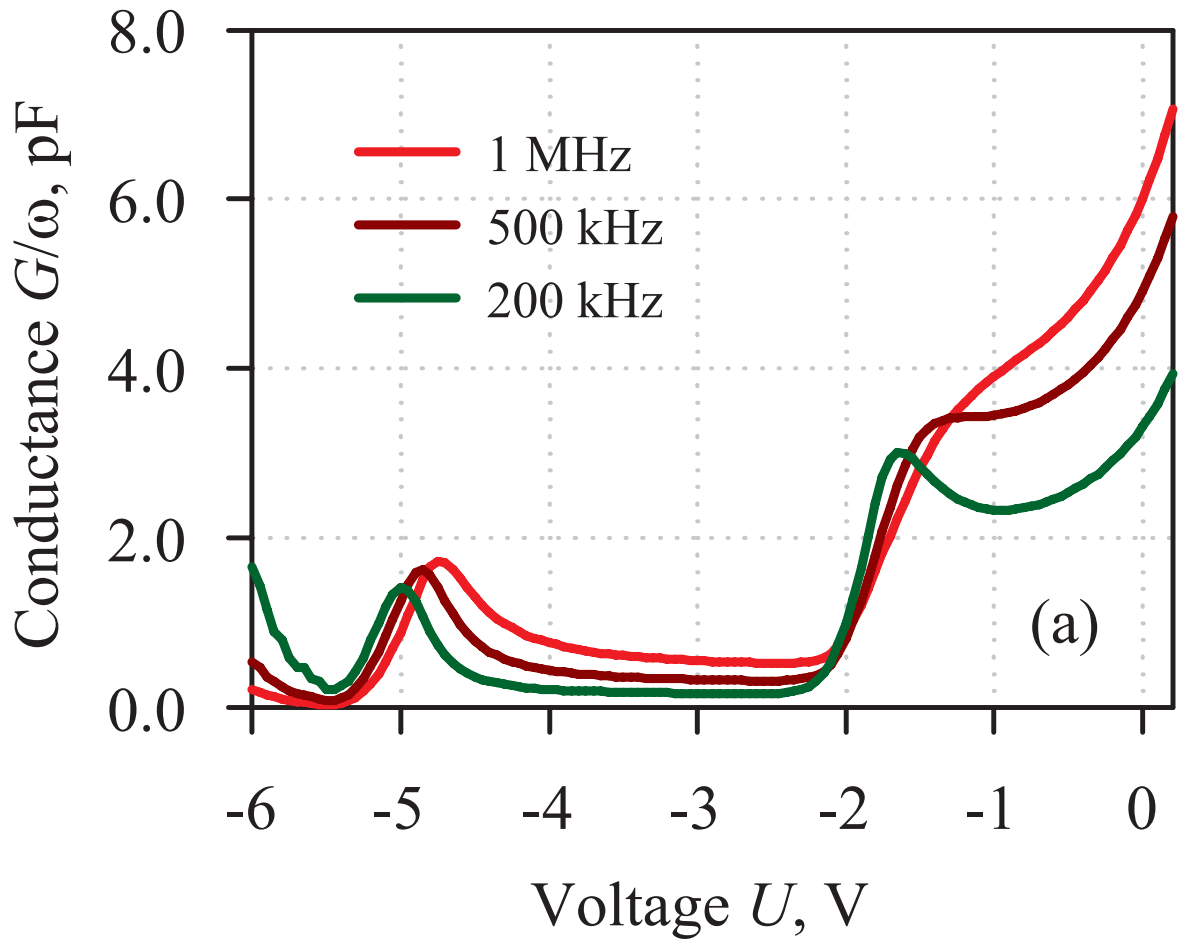


This is the author's peer reviewed, accepted manuscript. However, the online version of record will be different from this version once it has been copyedited and typeset.
 PLEASE CITE THIS ARTICLE AS DOI: 10.1063/1.50056842



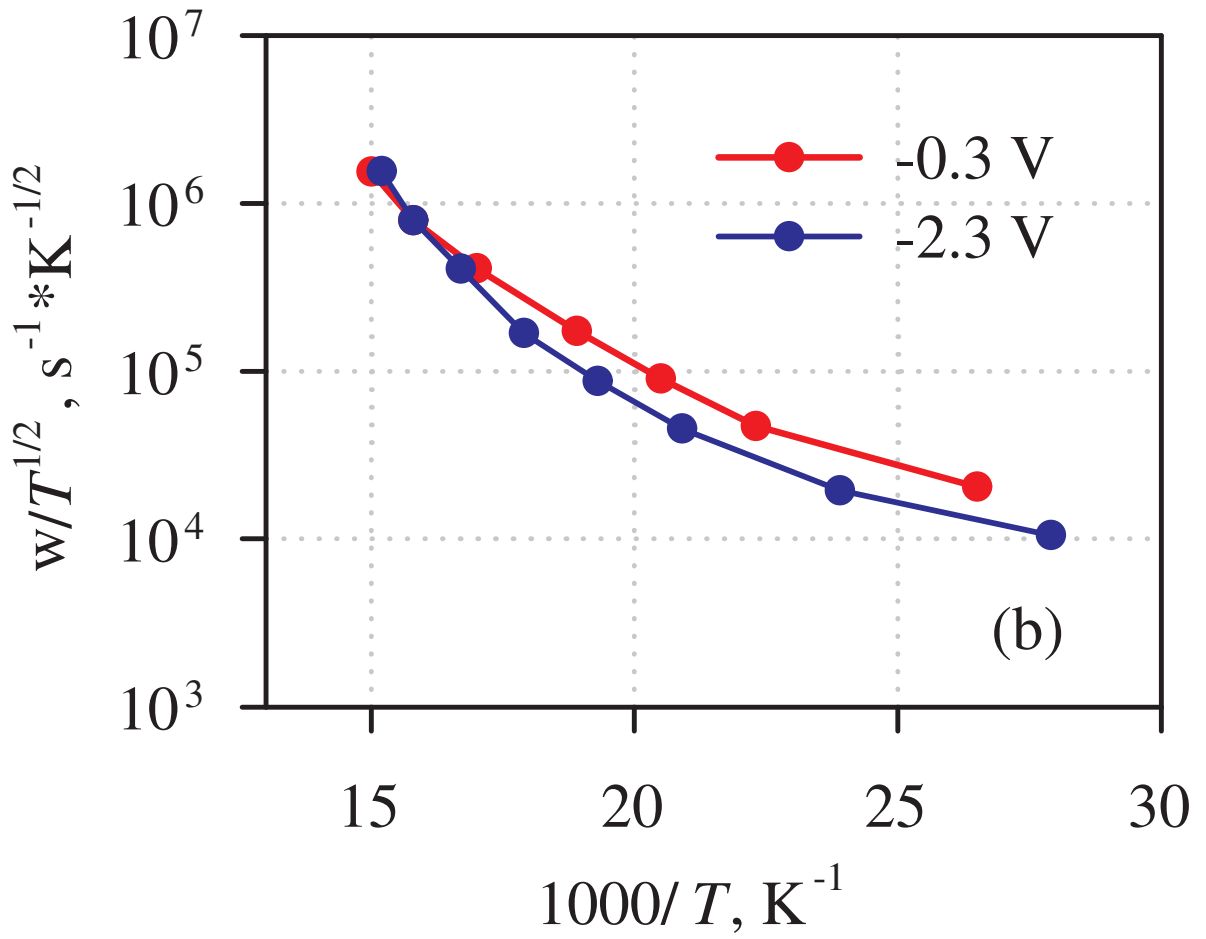
This is the author's peer reviewed, accepted manuscript. However, the online version of record will be different from this version once it has been copyedited and typeset.

PLEASE CITE THIS ARTICLE AS DOI: 10.1063/1.50056842

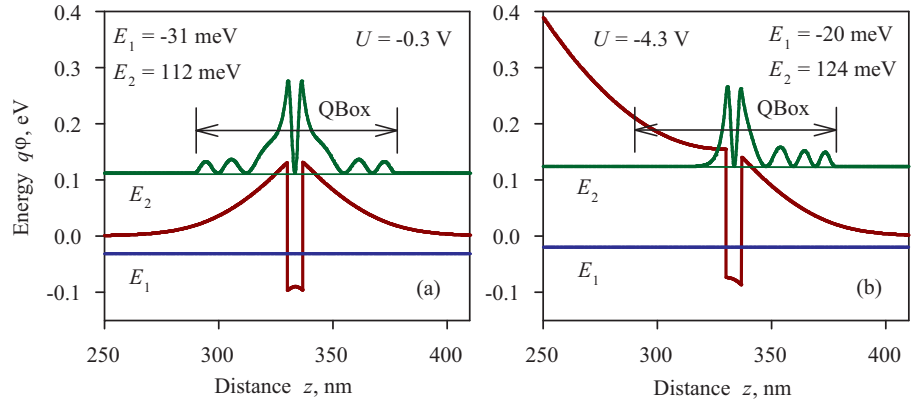


This is the author's peer reviewed, accepted manuscript. However, the online version of record will be different from this version once it has been copyedited and typeset.

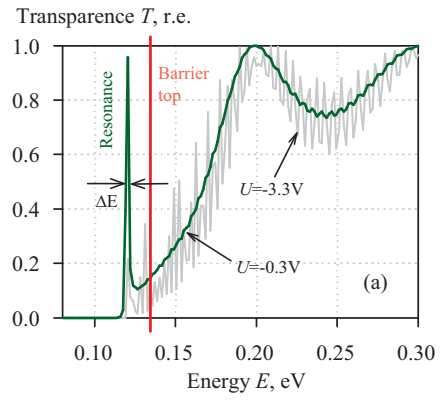
PLEASE CITE THIS ARTICLE AS DOI: 10.1063/1.50056842



This is the author's peer reviewed, accepted manuscript. However, the online version of record will be different from this version once it has been copyedited and typeset.
 PLEASE CITE THIS ARTICLE AS DOI: 10.1063/1.50056842



This is the author's peer reviewed, accepted manuscript. However, the online version of record will be different from this version once it has been copyedited and typeset.
 PLEASE CITE THIS ARTICLE AS DOI: 10.1063/1.50056842



This is the author's peer reviewed, accepted manuscript. However, the online version of record will be different from this version once it has been copyedited and typeset.

PLEASE CITE THIS ARTICLE AS DOI: 10.1063/1.50056842

